

the ESO Workshop, Käuffl, H.U. and Siebenmorgen, R. (Ed.) Springer-Verlag, 89–94.

²³Currie, D., D. Le Mignant, B. Svensson, E. Diolaiti, S. Tordo, K. Naesgarde, J. Liwing, O. Bendinelli, G. Parmeggiani, D. Bonaccini "Hyper-Velocity Jets and Homuncular Motion in eta Carinae: an

Application of the Fabry-Perot, ADONIS and AO Software" SPIE Vol. 4007 AO Systems Technology Editor: P. Wizinowich, # 4007–75, 1–12 (in press) (2000a)+

²⁴Christou, J. and Bonaccini, D. "An Analysis of ADONIS Data, tau Canis majoris – Deconvolution".

<http://www.lis.eso.org/lasilla/Telescopes/360cat/adonis/html/dated.html#idac>
²⁵Hester, J.J.; Light, R.M., Westphal, J.A., Currie, D.G., Groth, E.J.; Holtzmann, J.A., Lauer, T.R., O'Neil, E.J., Jr. "Hubble Space Telescope imaging of Eta Carinae" 1991 AJ 102, 654–657.

STARFINDER: a Code to Analyse Isoplanatic High-Resolution Stellar Fields

E. DIOLAITI¹, O. BENDINELLI¹, D. BONACCINI², L. CLOSE², D. CURRIE², G. PARMEGGIAN³

¹Università di Bologna – Dipartimento di Astronomia; ²ESO;

³Osservatorio Astronomico di Bologna

1. Introduction

StarFinder is a code designed to analyse Adaptive Optics images of very crowded fields. A typical AO observation has a well-sampled and complex-shape PSF, showing a sharp peak, one or more fragmented diffraction rings and an extended irregular halo. The approach followed in StarFinder (Diolaiti et al., 1999a, 1999b, 2000) is to analyse the stellar field with a digital image of the PSF, without any analytic approximation.

Under the assumptions of isoplanatism and well-sampling, StarFinder models the observed stellar field as a superposition of shifted scaled replicas of the PSF lying on a smooth background due to faint undetected stars, possible faint diffuse objects and noise.

The procedure derives first a PSF digital template from the brightest isolated field stars; then a catalogue of presumed objects is formed, searching for the relative intensity maxima in the CCD frame.

In the following step the images of the suspected stars are analysed in order of decreasing luminosity; each suspected object is accepted on the basis of its correlation coefficient with the PSF template; the relative astrometry and photometry of the source are determined by means of a fit, taking into account the contribution of the local non-uniform background and of the already detected stars.

At the end of the analysis it is possible to remove the contribution of all the stars detected up to this point and perform a new search for previously lost objects (e.g. secondary components of close binaries).

StarFinder is not a general-purpose algorithm for object recognition: it should be intended as a tool to obtain high-precision astrometry and pho-

tometry in adequately sampled high-resolution images of crowded stellar fields. In practice it can be applied not only to high-Strehl AO observations, but also to low-Strehl images. The code versatility has been also proved by an application to a set of HST NICMOS images (Section 3.3); in Aloisi et al. (2000) there is a comparison between our results and those obtained by DAOPHOT.

Much more intriguing and difficult to solve is the case of a field with space variant PSF, due to anisoplanatic effects in AO observations. In general the analysis of an anisoplanatic field requires the knowledge of the local PSF. The extension of StarFinder to the space variant case is in progress. Preliminary results have been presented at the ESO/SPIE meeting Astronomical Telescopes and Instrumentation 2000 (Diolaiti et al., 2000).

2. Analysis Procedure

2.1 PSF determination

The PSF is treated as a template for all the stars in the isoplanatic patch, so its knowledge is of basic importance for a reliable analysis.

The PSF extraction procedure included in StarFinder is based on the median average of a set of suitable stars selected by the user. Before being combined they are cleaned from the most contaminating sources, background-subtracted, centred with sub-pixel accuracy and normalised. The centring is performed by an iterative shift of the stellar image in order to cancel the sub-pixel offset of its centroid. The halo of the retrieved PSF is then smoothed, applying a variable box-size median filtering technique.

The PSF extraction procedure is able to reconstruct approximately the core of

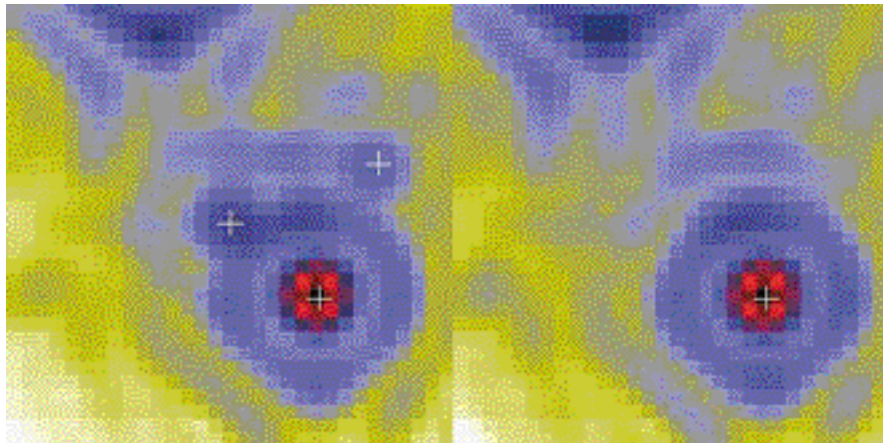


Figure 1: Left: sub-image extracted from a (simulated) stellar field, including the central star to be analysed, a brighter source which is already known, a fainter one, which will be examined later, and the PSF feature of a much brighter star, represented by the structure in the upper-left part of the sub-image. Right: corresponding sub-region extracted from the stellar field model, containing one replica of the PSF for each star detected so far.

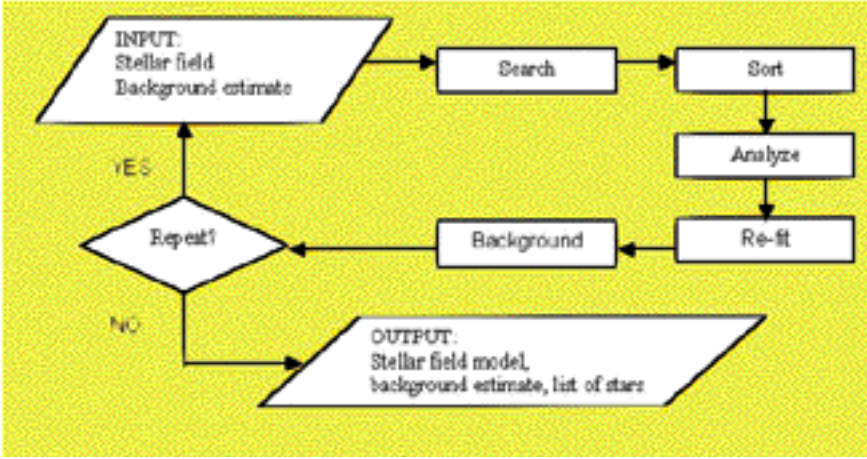


Figure 2. Flow-chart of the algorithm for star detection and analysis.

saturated stars, replacing the corrupted pixels with the central part of a preliminary estimate of the PSF: accurate positioning is accomplished by means of a cross-correlation technique, whereas the scaling factor is determined with a least squares fit to the wings of the star that is analysed.

2.2 Standard analysis of the stellar field

The starting point is a list of presumed stars, including the relative maxima which fulfil the detection condition

$$i(x, y) > b(x, y) + t, \quad (1)$$

where $i(x, y)$ is the observed intensity, $b(x, y)$ the background emission and t a detection threshold, which may be chosen as a function of the noise standard deviation. Preliminary image smoothing reduces the incidence of noise spikes.

The presumed stars are listed by decreasing intensity and analysed one by one. In order to illustrate a generic step of the algorithm, we assume that the first n objects have already been examined and that a suitably scaled and positioned replica of the PSF has been put in a 'synthetic stellar field' for each star detected up to this point. We consider now the $(n+1)$ -th object in the list. First of all, a small sub-image of fixed size is extracted around the object (Fig.1, left). Notice that the actual box size is comparable to the diameter of the first diffraction ring of the PSF, then smaller than shown in Figure 1; the only purpose of this picture is to illustrate a typical situation occurring in the analysis of a stellar field.

This region of interest may contain brighter stars already analysed, fainter objects neglected in the current step and PSF features of other stars lying both within or outside the sub-image support. The information on the brighter sources is recorded in a synthetic stellar field model (Fig. 1, right), defined as the sum of two terms: a superposition of PSF replicas, one for each star de-

tected up to this point, and an estimate of the background emission, assumed to be non uniform in general.

The complexity of the PSF features might lead to spurious detections: to assess the reliability of the object of interest (the relative maximum at the centre of the left panel in Figure 1), we subtract the contribution of the background and of the brighter stars, derived from the synthetic field (Fig.1, right).

If a statistically significant residual can still be identified, it is compared to the PSF with a correlation check, as an objective measure of similarity. The correlation coefficient is computed on the central spike of the diffraction pattern is considered, out to the first dark ring. A correlation threshold (e.g. 0.7–0.8) must be fixed in order to discriminate and reject unlikely detections. The correlation coefficient represents also an effective tool to select, among the detected stars, the ones with the highest photometric reliability, since a very high correlation value is generally associated to resolved single sources.

The object in hand is accepted only if the correlation coefficient is greater than the selected level, and its position and flux are obtained by means of a local fit. Taking into account the contribution of the bright stars outside the fitting region known from the synthetic field, a slanting plane representing the local background and a sum of shifted weighted replicas of the local PSF, one for each point-source identified in the fitting region. Sub-pixel astrometric accuracy is achieved by a non-linear optimization of the star positions, which is based on the interpolation of the given PSF array. If the fit is acceptable the star field catalogue and the related synthetic image are upgraded by the new entry.

The basic step described above (detection of the suspected stars and analysis) may be repeated: a new list of presumed stars is formed after subtracting the previously detected ones and the analysis is started again on the original

image. This iteration is very useful to detect stars in crowded groups, down to separations comparable to the Rayleigh limit for the detection of close binaries.

An optional deblending mode is available. All the objects somewhat more extended than the PSF are considered blends. The measurement of the area is based on thresholding the object at a pre-fixed level below the peak, after subtracting the local background and the other known stars around. The deblending strategy consists of an iterative search for residuals around the object and subsequent fitting; the iteration stops when no more residual is found or the fit of the last residual was not successful.

The flow-chart in Figure 2 represents the main loop of the algorithm, which can be iterated any number of times. In practice after 2–3 iterations the number of detected stars approaches a stable value.

2.3 PSF enhancement

At the end of the overall analysis, it is possible to run again the PSF extraction procedure, exploiting the upgraded estimates of the image background and of the contaminating sources around the PSF stars: this should allow a better determination of the PSF. Then a more accurate analysis can be performed.

2.4 Fitting procedure

The fitting technique treats the PSF as a template which may be scaled and translated. A sub-image centred on the star of interest is extracted and approximated with the model

$$h(x, y) = s_0(x, y) + \sum_{n=1}^{N_s} p(x-x_n, y-y_n) + b_0 + b_1 x + b_2 y, \quad (2)$$

where $s_0(x, y)$ is the fixed contribution of known stars outside the sub-image support, N_s is the number of point sources within the sub-image, x_n, y_n, f_n are the position and flux of the n -th source, $p(x, y)$ is the PSF and b_0, b_1, b_2 are the coefficients of a slanting plane representing the local background.

The optimisation of the parameters is performed by minimising the least squares error between the data and the model, with an iterative Newton-Gauss technique, which requires the computation of the model derivatives. For this purpose the Fourier shift theorem is applied to the PSF:

$$p(x - y_n, y - y_n) = FT^{-1} \{ FT \{ p(x, y) \} e^{-i2\pi(ux_n + vy_n)/N} \} \quad (3)$$

where FT is the discrete Fourier transform, N is the sub-image size and u, v are spatial frequencies. The derivative with respect to x_n is

$$\frac{\partial p(x - x_n, y - y_n)}{\partial x} = \mathcal{FT}^{-1} \left[\mathcal{FT} [p(x, y)] \exp[-i2\pi(xu + yv)] \mathcal{FT} \left[-i \frac{2\pi u}{\lambda} \right] \right] - \mathcal{FT}^{-1} \left[\left(-i \frac{2\pi u}{\lambda} \right) \mathcal{FT} [p(x - x_n, y - y_n)] \right]$$

and requires in practice an interpolation of the PSF to compute $p(x - y_n, y - y_n)$. This operation may be performed, for instance, with the cubic convolution interpolation implemented in the IDL

function *interpolate*. A similar algorithm has been described by Véran *et al.* (1998).

In principle this method can only be applied to well-sampled images,

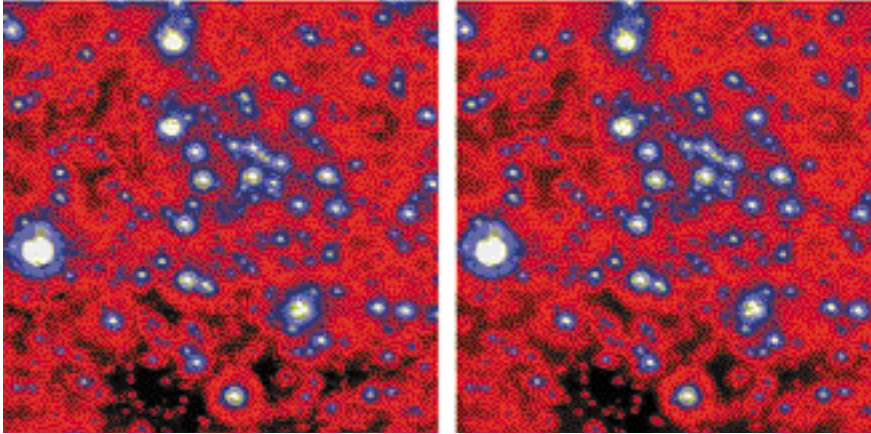


Figure 3: Left: PUEO image of the Galactic centre. Right: reconstructed image, given by the sum of about 1000 detected stars, and the estimated background. The display stretch is square root.

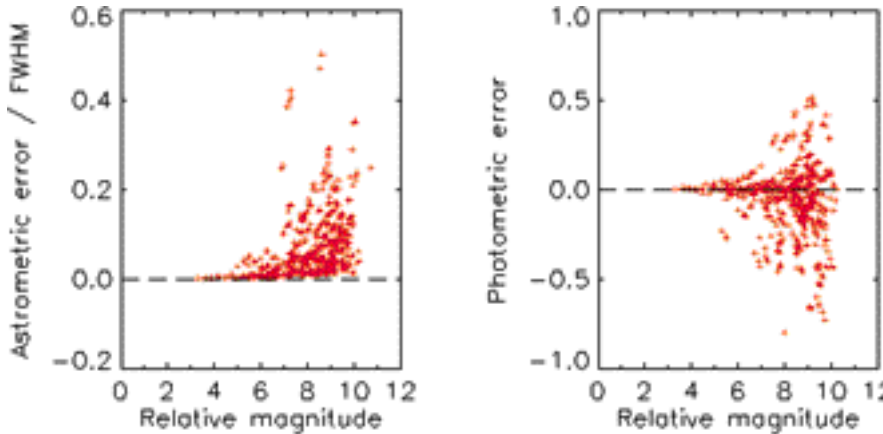


Figure 5: Left: plot of astrometric errors vs. relative magnitude of detected synthetic stars; the errors are quoted in FWHM units (1 FWHM \sim 4 pixels) and represent the distance between the true and the calculated position. Right: plot of photometric errors. A tolerance of 1 PSF FWHM has been used to match each detected star with its true counterpart.

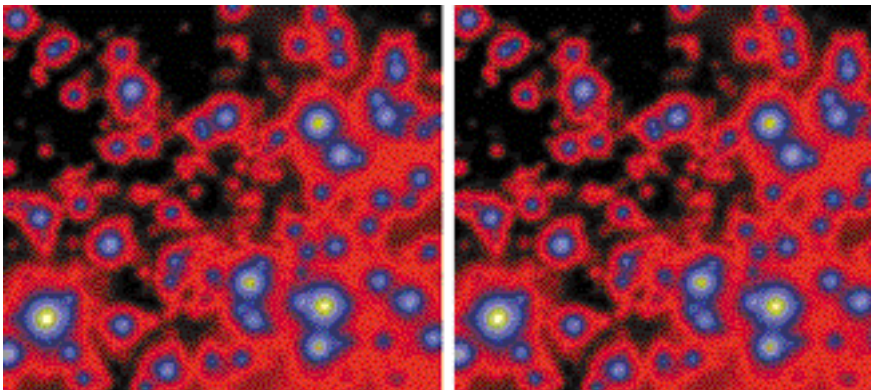


Figure 6: Left: 47 Tuc observed image. Right: reconstructed image. The display stretch is log arithmetic.

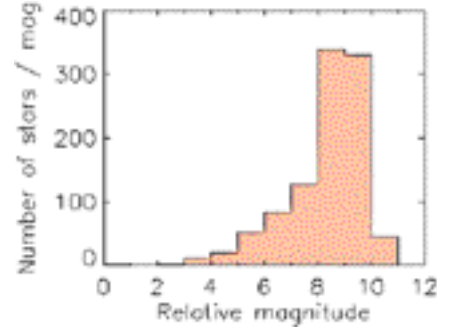


Figure 4. Galactic centre: estimated luminosity function.

even though tests on under-sampled data are producing encouraging results.

3. Applications

3.1 High Strehl case

The code has been run on a K-band PUEO image of the Galactic centre (Fig. 3, left), kindly provided by François Rigaut. This image is an example of a well-sampled high-Strehl AO observation of a stellar field.

The total field of view is about 13×13 arcsec² and the pixel size 0.035 arcsec. The PSF is stable across the image, apart from some minor features especially on the shape of the first diffraction ring. We will show that assuming a constant PSF it is possible to obtain accurate results.

About 1000 stars have been detected, with a correlation coefficient of at least 0.7; the reconstructed image is shown in Figure 3, right.

We have evaluated the astrometric and photometric accuracy of the code by means of an experiment with synthetic stars: for each magnitude bin in the retrieved luminosity function (Fig. 4), a total of 10% synthetic stars at random position have been added to the image. In practice, 10 frames have been created with this procedure and analysed separately.

The catalogues of detected artificial stars for each frame have been merged together; then the astrometric and photometric errors have been computed and plotted as a function of the true magnitude (Fig. 5).

The plots show accurate astrometry and photometry and there is no apparent photometric bias.

3.2 Low Strehl case

A low-Strehl example is represented by the H-band image of the globular cluster 47 Tuc, observed at the ESO 3.6-m telescope with the ADONIS AO system (Fig. 6). The image is very well sampled with a FWHM of \sim 6 pixels (1 pixel = 0.1 arcsec).

As in the previous high-Strehl case, we have evaluated the accuracy of the algorithm by means of an experiment

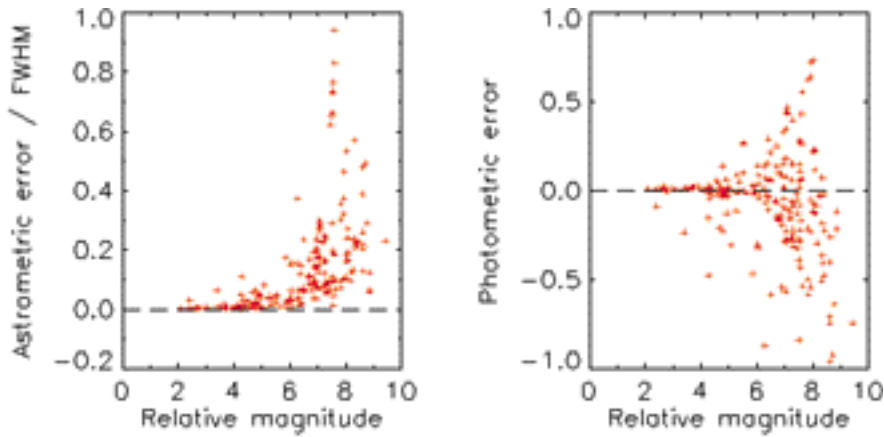


Figure 7: Left: plot of astrometric errors vs. relative magnitude of detected synthetic stars; the errors are quoted in FWHM units (1FWHM \sim 6 pixels) and represent the distance between the true and the calculated position. Right: plot of photometric errors. A tolerance of 1 PSF FWHM has been used to match each detected star with its true counterpart.

with synthetic stars. The astrometric and photometric errors for the detected artificial sources are shown in Figure 7.

3.3 HST image

The last application concerns a HST observation of the starburst galaxy NGC 1569, observed with the NICMOS camera in the F110 W and F160 W filters, roughly corresponding to the standard J and H bands. The originally under-sampled dithered frames have been combined with the Drizzle code, obtaining two well-sampled images which have

been analysed independently (Aloisi et al., 2000). In the F160 W frame, thanks to the finer sampling of the PSF, it has been possible to apply the de-blending strategy based on the recognition of blends by their larger extension as compared to the PSF. The two images, along with the corresponding reconstruction, are shown in Figure 8.

The lists of the detected stars have been compared by matching the corresponding reference frames and retaining all the objects with a relative offset smaller than 1/2 pixel. A subset of the 3133 retrieved common stars

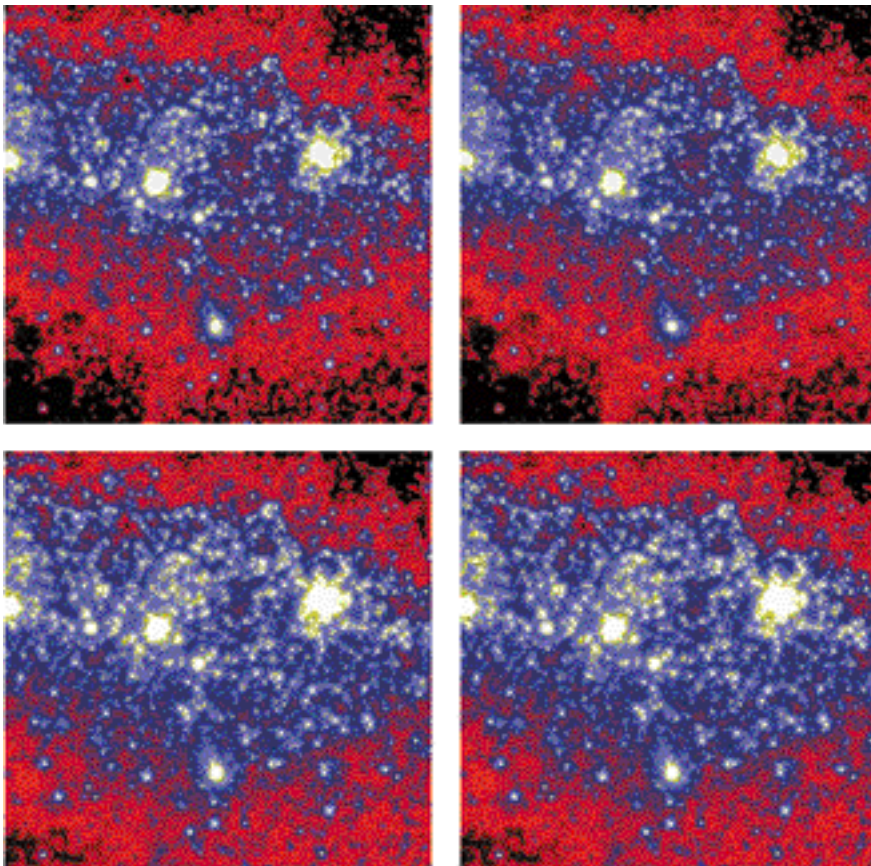


Figure 8: NGC 1569. Top: F110 W band, observed and reconstructed image. Bottom: F160 W band, the same. The display stretch is logarithmic.

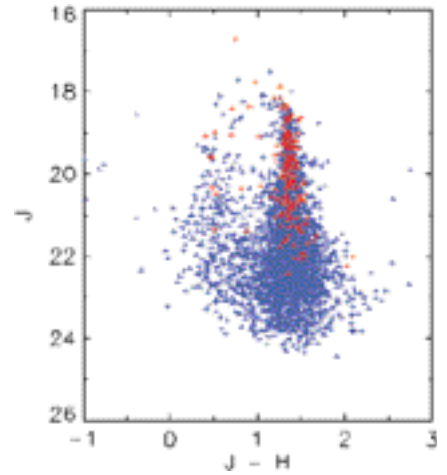


Figure 9. The NGC 1569 CMD diagram. Blue and red crosses: complete set; red crosses: stars with high correlation coefficient.

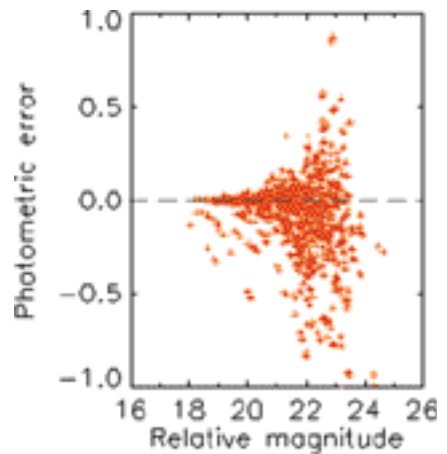


Figure 10: Photometry accuracy plot.

has been created selecting the sources with a very high (more than 0.975) correlation coefficient: high values of this parameter are generally associated to resolved single stars. The complete set of 3133 objects (blue and red crosses) and the selected one including 195 stars (red crosses), are shown in Figure 9.

The photometric accuracy has been evaluated by means of an experiment with synthetic stars, similar to those performed in the previous applications. The photometric errors for the successfully detected synthetic sources in the F110 W filter are plotted in Figure 10; similar results have been obtained for the F160 W frame. The slight bias toward negative errors may be attributed to the extreme crowding of this field: when a synthetic star falls on a fainter source, the latter might be lost whereas the luminosity of the former might be overestimated.

4. The IDL Code

The StarFinder code has been provided with a collection of auxiliary routines for data visualisation and basic

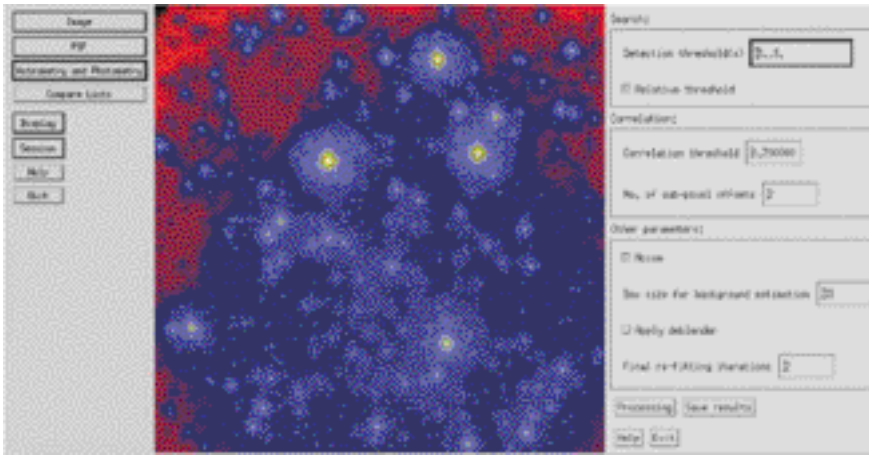


Figure 11: Widget based GUI interface.

image processing, in order to allow the user to analyse a stellar field, produce an output list of objects and compare different lists, e.g. referred to different observations of the same target. The input image is supposed to be just calibrated. The code is entirely written in the IDL language and has been tested on Windows and Unix platforms supporting IDL v. 5.0 or later. A widget-based graphical user interface has been created (Fig. 11). The main widget appearing on the computer screen is an interface to call secondary widget-based applications, in order to perform various operations on the image. The basic documentation about the code can be found in the on-line help pages and in the attached manual. IDL users

might wish to run interactively the StarFinder routines, without the widget facilities: complete documentation on each module is available for this purpose. A copy of StarFinder can be obtained in the Web page of the Bologna Observatory (www.bo.astro.it) or by contacting the writer and maintainer of the code (E.D.) at the e-mail address diolaiti@bo.astro.it

5. Conclusions

The elaboration of real and simulated data seems to prove the effectiveness of StarFinder in analysing crowded stellar fields characterised by high Strehl ratio PSFs and correct sampling, reaching in this case the full utilisation of the

data information content. The code can be applied also to low Strehl or under-sampled data with results comparable to those attainable by other methods. StarFinder is also reasonably fast: the analysis of a field comparable to the Galactic centre image requires between 5 and 10 minutes on a normal PC (Pentium Pro-64 Mb-350 MHz).

The first improvement of StarFinder, available in a near future, will allow to analyse star fields with space variant PSF.

Acknowledgements

François Rigaut is acknowledged for kindly providing the PUEO image of the Galactic centre and for supporting the initial development of this method.

References

- Aloisi A. et al., 2000. In preparation.
- Diolaiti E. et al., 1999a, "An algorithm for crowded stellar fields analysis", in *Astronomy with Adaptive Optics: present results and future programs*, Sonhofen, ESO Conf. and Workshop Proc. No. 56, p.175.
- Diolaiti et al., 1999b, "StarFinder: a code for crowded stellar fields analysis" in *ADASS IX*, Hawaii. In press (astro-ph/9911354).
- Diolaiti E. et al., 2000, "StarFinder: an IDL GUI based code to analyze crowded fields with isoplanatic correcting PSF fitting", in *Adaptive Optical System Technology*, Munich. In press (astro-ph/0004101).
- Véran J.-P. et al., 1997, *J. Opt. Soc. Am. A*, **14** (11), 3057.
- Véran J.-P., Rigaut F., 1998, *Proc. SPIE* **3353**, 426.

VLT Laser Guide Star Facility: First Successful Test of the Baseline Laser Scheme

D. BONACCINI^a, W. HACKENBERG^a, R.I. DAVIES^b, S. RABIEN^b, and T. OTT^b

^aESO, Garching; ^bMax-Planck-Institut für Extraterrestrische Physik, Garching

The planned baseline laser for the VLT Laser Guide Star Facility (LGSF) consists of dye laser modules, capable of producing > 6.5 W CW each (1). Two such modules can fit on a 1.5 × 1.5 m optical table. The laser concept was developed in a preliminary LGSF study phase (2) and is a variation of the ALFA laser (3) used in Calar Alto (Spain). It uses two Coherent Inc. all-solid state Compass Verdi 10 W lasers at 532 nm, to pump a modified Coherent model 899-21, continuous-wave (cw) ring-dye laser. The dye is Rhodamine 6G (Rh6G).

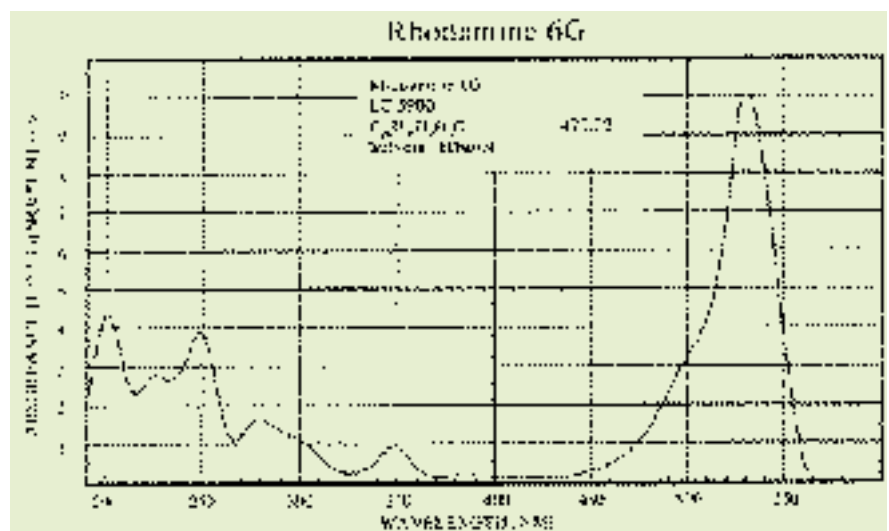


Figure 1: Absorption profile of the laser dye, Rhodamine 6G.